ACS OMEGA

http://pubs.acs.org/journal/acsodf

Article

Unravelling Binding of Human Serum Albumin with Galantamine: Spectroscopic, Calorimetric, and Computational Approaches

Ghulam Md Ashraf,* Debarati Das Gupta, Mohammad Zubair Alam, Saleh Salem Baeesa, Badrah S. Alghamdi, Firoz Anwar, Thamer M. A. Alqurashi, Waleed Al Abdulmonem, Mohammed A. Alyousef, Fahad A. Alhumaydhi, and Anas Shamsi

Cite This: *ACS Omega* 2022, 7, 34370−34377

Read Online

ACCESS | Metrics & More | Article Recommendations | Supporting Information

ABSTRACT: Human serum albumin (HSA), an abundant plasma protein, binds to various ligands, acting as a transporter for numerous endogenous and exogenous substances. Galantamine (GAL), an alkaloid, treats cognitive decline in mild to moderate Alzheimer's disease and other memory impairments. A vital step in pharmacological profiling involves the interaction of plasma protein with the drugs, and this serves as an essential platform for pharmaceutical industry advancements. This study is carried out to understand the binding mechanism of GAL with HSA using computational and experimental approaches. Molecular docking revealed that GAL preferentially occupies Sudlow's site I, i.e., binds to subdomain IIIA. The results unveiled that GAL binding does not induce any conformational change in HSA and hence does not compromise the functionality of HSA. Molecular dynamics simulation (250 ns) deciphered the stability of the HSA−GAL complex. We performed the fluorescence binding and isothermal titration calorimetry (ITC) to analyze the actual binding of GAL with HSA. The results suggested that GAL binds to HSA with a significant binding affinity. ITC measurements also delineated thermodynamic parameters associated with the binding of GAL to HSA. Altogether, the present study deciphers the binding mechanism of GAL with HSA.

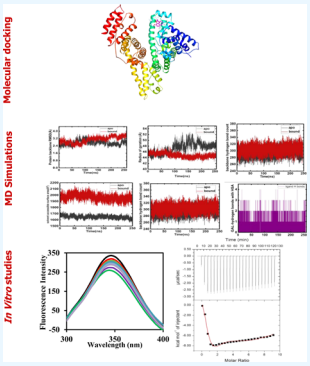

1. INTRODUCTION

Drug−protein interactions are important for drug discovery because they provide a platform for the drug's availability, efficiency, and transport.[1,2] Many studies have used human serum albumin (HSA) as a model protein for drug−protein interactions because pharmacological profiling of a drug is influenced by how it binds to HSA.[3] HSA performs a wide range of functions; it can bind to an extensive array of exogenous and endogenous chemical molecules,[4] including drugs, fatty acids, nucleic acids, hormones, metals, and toxins, thereby acting as the primary carrier of all these.[5,6] HSA is the key player in oncotic pressure and fluid distribution between body compartments.[7,8] Physiologically, HSA regulates colloid osmotic pressure and may affect microvascular integrity and inflammatory pathway aspects, namely, neutrophil adhesion and others.[9] HSA is also involved in heme scavenging. It acts as a carrier of the macrocycle; i.e., the transfer of macrocycle from high- and low-density lipoproteins to hemopexin is carried out by HSA.[10] Drugs that are poorly soluble in water bind to HSA in the bloodstream and get delivered to target tissues, highlighting the importance of HSA. The importance of HSA is attributable to being a vital biomarker of diseases ranging from cancer to obesity, diabetes, and others.[11−14] It also has clinical applications in treating various pathologies, acute liver failure, chronic liver disease, and others.[15,16]

HSA, 585 amino acids long, is primarily a helical protein (67% α-helix), having 17 disulfide bonds, 1 free thiol group, and 1 one Trp (Trp-214) residue.[14,17] Structurally, it comprises three physically identical domains (I, II, and III), and each domain is divided into two subdomains (A and B) sharing common structural elements; Trp 214 is present in the domain IIA of HSA.[18] There are many drug-binding sites in HSA, but primarily drugs bind to two sites, one in subdomain IIA, Sudlow site 1, and the other in the subdomain IIIA, Sudlow site 2.[19]

Neurodegenerative diseases are connected to the cholinergic system; acetylcholine is the main neurotransmitter broken by acetylcholinesterase (AChE). Hence, AChE inhibitors and muscarinic and nicotinic receptor (nAChR) agonists are employed for these disorders.[20] According to the literature, it is generally assumed that AChE inhibitors or nicotinic and muscarinic receptor agonists improve cholinergic function, a pathological feature observed in Alzheimer's disease (AD). These inhibitors do not cure AD; instead, they improve the patient's life, but the shortcoming is that this therapy is symptomatic, that is, symptom onset is deferred and not a whole cure.[21,22]

Received: June 27, 2022
Accepted: August 10, 2022
Published: September 19, 2022

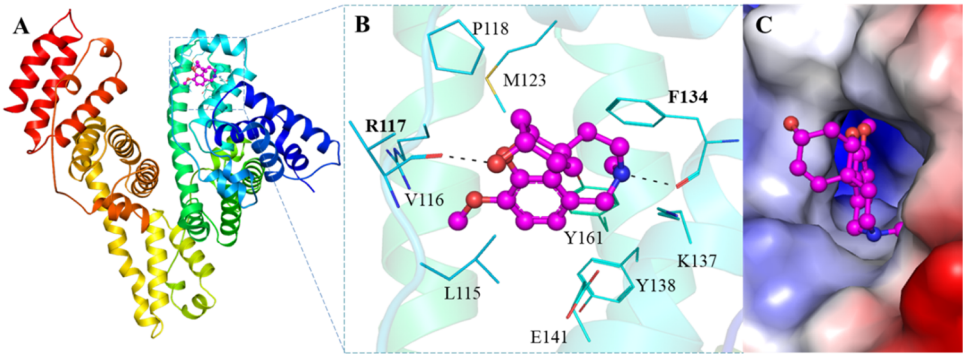

Figure 1. Molecular interactions of HSA with GAL. (A) Cartoon structural representation, (B) interacting residues, and (C) potential surface cavity representation of HSA residues interacting with GAL.

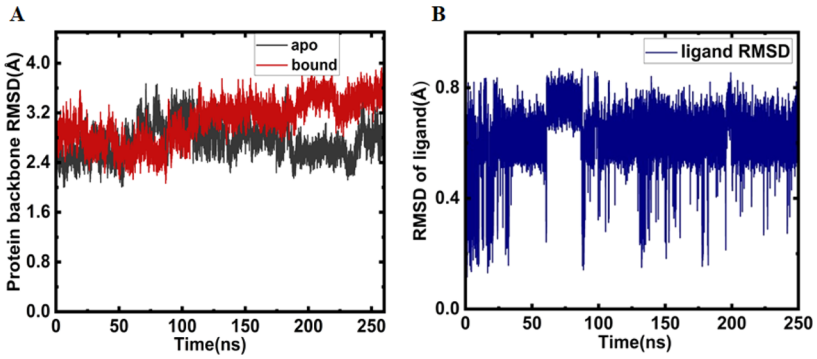

Figure 2. (A) RMSD fluctuations of the protein backbone, bound (red) and free (black) HSA during 250 ns production. (B) RMSD of ligand during the production runs.

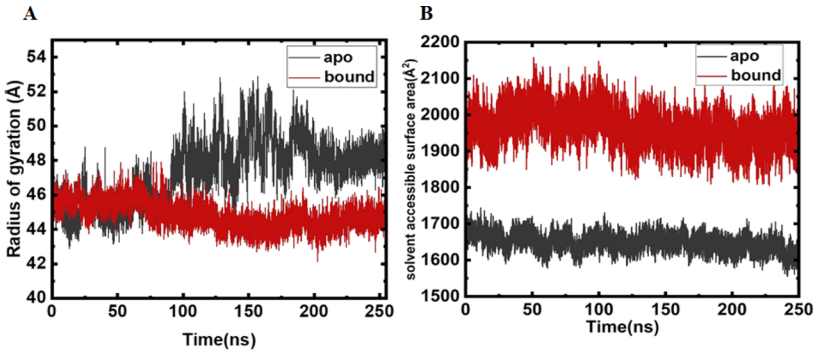

Figure 3. (A) R_g for GAL-bound HSA plotted as a function of snapshots. (B) SASA plotted as a function of snapshots.

Galantamine (GAL), a moderate AChE inhibitor, belongs to tertiary plant alkaloids and is recommended for treating mild to moderate AD forms. It is a selective AChE inhibitor because its inhibition is regulated by dose; it has 53-fold stronger selectivity for action on AChE than BChE. According to recent studies, GAL does not affect nAChR. Studies have reported that GAL shows beneficial effects due to inhibition of AChE and other mechanisms without nAChR activation.[23] GAL improves cognitive function in severe AD patients, but the overall general status of the patient is not affected much.[24] Besides its positive implications for cognition function, GAL also reduces mortality.[25]

This study was carried out to understand the binding of GAL with HSA. Molecular docking suggested that GAL binds to HSA with an appreciable affinity. Molecular dynamics (MD) simulation studies were performed to comprehend the structural flexibility and conformational dynamics behavior of the HSA−GAL system. Fluorescence binding further confirmed the actual binding of GAL to HSA with a good affinity. The present work unveils GAL binding with HSA, establishing that GAL binds to HSA with a significant affinity, forming a stable HSA−GAL complex.

2. RESULTS

2.1. Molecular Docking. The molecular docking results were examined to explore the plausible binding of GAL with HSA. Molecular docking revealed that GAL interacts with HSA with an appreciable −7.4 kcal/mol affinity. GAL preferentially occupies the Sudlow site I, between domain IA and IIB of HSA (Figure 1A). It directly interacts with various functional residues of HSA, including Arg117 and Phe134 (Figure 1B). The interaction analysis of the docked complex suggested that GAL interacts with many functionally active residues. At the same time, various other residues of the HSA

https://doi.org/10.1021/acsomega.2c04004
ACS Omega 2022, 7, 34370−34377

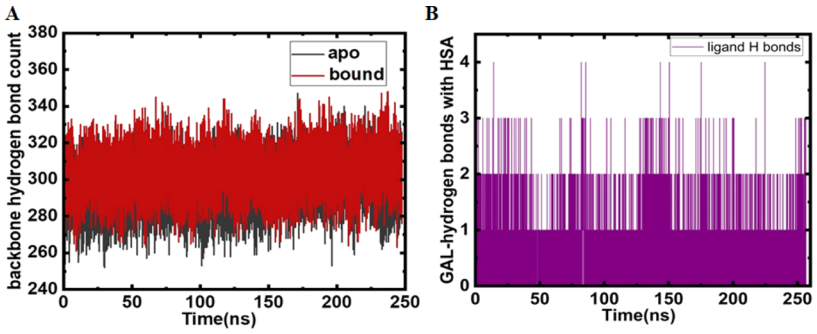

Figure 4. (A) HSA intramolecular hydrogen bonds (H bonds) monitored during 250 ns production runs (GAL-bound HSA). (B) Intermolecular hydrogen bond analysis of HSA−GAL complex.

binding pocket, such as Leu115, Val116, Pro118, Met23, Lys137, Tyr138, Glu141, and Tyr161, shared various hydrophobic interactions with GAL (Figure 1B). GAL resides in the deep binding pocket cavity critical for HSA activity (Figure 1C). Substantial interactions between HSA and GAL suggest their strong binding partnership.

2.2. Structural Changes and Analyses Post-MD. When small molecules bind to proteins, it causes significant conformational fluctuations, and MD simulations are vital to probe these phenomena atomistically. Various studies have deployed MD to investigate these fluctuations.[26,27]

2.2.1. Root Mean Squared Deviations. A powerful tool to investigate residue-based fluctuations is root mean squared deviations (RMSD). We calculated the RMSD of apo and ligand-bound proteins to compare these dynamics (Figure 2A). The RMSD plot demonstrates the stability of the protein, and the average RMSD ranges between 2.8 and 3 Å. Gal binding seems to enhance the stability of the complex, and the figure clearly shows the bound simulation RMSD to be slightly lower than the apo simulations. The ligand's RMS fluctuations are monitored to track the ligand's conformations during the 250 ns MD runs. Figure 2B clearly shows that GAL RMSD is ∼0.6 Å and resides in the docked pocket during MD progression.

2.2.2. Radius of Gyration (R_g). The radius of gyration (R_g) is an important marker that detects compactness in the protein's tertiary structure. It is the RMS distance of the set of atoms from their collective center of mass. R_g of the apo and GAL-bound HSA is shown in Figure 3A. The R_g of bound HSA shows compaction in the last 100 ns of the 250 ns trajectory. The apo simulations show that the R_g stays stable between 0 and 70 ns, then slightly increases between 100 and 140 ns, showing adjustment in overall structure, relaxation, and expansion. Finally, in the latter 60 ns of the trajectory, the Radius of gyration remains stable with an average value of 48 Å. The R_g of GAL-bound HSA shows compaction in the last 100 ns of the 250 ns trajectory, and the value is slightly lesser than the apo simulation data.

2.2.3. Solvent Accessible Surface Area. Solvent accessible surface area (SASA) is a useful metric to post-process MD results. SASA values were calculated and plotted to determine the impact of GAL binding on the solvent accessibility of HSA (Figure 3B). The plot shows a minor increase in the SASA values of bound HSA when complexed with apoprotein. Overall, the SASA values show a fair equilibration during the last 100 ns without any significant switching throughout the simulation. A careful look at the SASA plots gives a better picture of the atomistic data. In the bound simulation data (red), the SASA values show an increase compared to apo data. This means that the residues in the protein change rearrange and reorganize the global foldedness, which reflects in the higher SASA values. In the latter half of the trajectory, the values plateau out and seem to closely track with the apo SASA data. Thus, the reorganization in the protein chain is demonstrated in the SASA plots.

2.2.4. Hydrogen Bond Analysis. The main goal of analyzing the hydrogen bond formation was to evaluate the biomolecule's stability and verify that the native structure is not distorted or artifacts are produced due to the simulation protocol. Investigating the number of intramolecular hydrogen bonds provides a platform to analyze structures' stability during MD simulations. Figure 4A shows intramolecular H bonds in HSA during production runs of GAL-bound structure. The protein core remains stabilized with minimal fluctuations. The average number of intramolecular H bonds fluctuates from 280 to 320 (Figure 4A).

The protein−ligand hydrogen bonds are essential two-dimensional (2D) fingerprint-based descriptors to probe key interactions of some residues with ligand atoms. We plotted the hydrogen bonds formed with GAL during the 250 ns production runs (Figure 4B). The hydrogen bonds formed with HSA and GAL vary between 1 and 3. The key binding site residues have a longer lifetime hydrogen bond interaction with the ligand, as evidenced by Figure 4B. The MD simulations show the pronounced hydrogen bonding in the HSA−ligand complex. Overall, the analysis advocates that the HSA−GAL complex is quite stable, and the simulation has been successful in computing various binding characteristics and non-bonded interactions of GAL with the protein of interest in this study.

2.3. Free Energy Calculations. Protein−ligand binding free energies are crucial as they aid in the selection of efficacious ligands from a myriad of different alternatives. In this study, we employed both molecular mechanics poisson Boltzmann (MMPBSA) and linear interaction energy (LIE) methodologies to compute binding affinities of GAL.

For computing the LIE estimates, we ran the single ligand in a box of TIP3P water. We then computed the net electrostatics and van der Waals values of the bound ligand interacting with the protein residues and the solvent, and the single ligand interacting with the solvent. The electrostatic value was scaled using b and the van der Waals were scaled using linear scaling constant a. We have used default values of both scaling factors, although some papers have reported optimized values for polyphenolic type ligands and other multiple hydroxylated ligands in literature.

https://doi.org/10.1021/acsomega.2c04004
ACS Omega 2022, 7, 34370−34377

$$\Delta E(\mathrm{LIE}) = \alpha (E_{\mathrm{bound}} - E_{\mathrm{unbound}})^{\mathrm{vdW}} + \beta (E_{\mathrm{bound}} - E_{\mathrm{unbound}})^{\mathrm{elec}}$$

The binding affinity value calculated for GAL is −7.92 kcal/mol.

The energies are plotted in Figure 5.

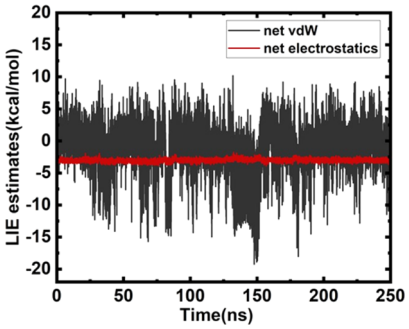

Figure 5. GAL binding affinity estimated via LIE methodology (electrostatics plotted in red and net van der Waals plotted in black).

Although immense efforts have been made in the regime of computational chemistry, computational prediction of free energies of binding remains a formidable challenge. Over the past 50 years, molecular mechanics generalized born surface area (MMGBSA) calculations have been an efficient and robust computational method for estimating protein−ligand binding energies. They are less computationally expensive than free energy perturbations and alchemical methods but way more technically sound and accurate than docking scoring functions. Due to this optimized performance over the past 5 decades, MMPBSA and MMGBSA have been widely used to evaluate docking poses, determine structural stability, and predict binding affinities and hotspots. In addition, MMPBSA and MMGBSA can be tweaked to compute contributions from each amino acid residue in the protein structure, which provides detailed residue-specific energetic contributions to the system binding. This helps drug discovery campaigns as the dominant free energy contributors can be parsed and fine-tuned to optimize new leads and drug-like fragments to the clinic.

In this work, we computed the binding affinities of GAL using MMPBSA as it is more computationally exhaustive and thus yields a more accurate free energy estimate than the GBSA analogue. We turned to AMBER's inbuilt LIE method to evaluate the binding affinity more confidently. It is an endpoint method that uses the MD simulations' snapshots to compute protein−ligand binding estimates. The total energy is a composite of electrostatics and van der Waals interactions, and independent scaling constants individually scale. The scaling constant (b) slightly varies between neutral and charged ligands and has been tested on various drug-like compounds. LIE has the advantage of computing not just protein−ligand interactions but also ligand−water interactions and using the ligand in a box of water simulation as its reference value. The LIE estimated value for GAL binding stands at −11.8 kcal/mol. MMGBSA reports the binding energy value at −16.2 kcal/mol (Table 1). The numbers were compared with the experimental IC50 values later in the study with good agreement.

2.4. Fluorescence Assay. With the aid of computational approaches, we have established that GAL binds to HSA with a good affinity, forming a stable complex over time. The actual binding of GAL with HSA was further validated by fluorescence binding assay. When an electron in a higher energy state returns to a lower energy state, fluorescence is observed owing to photon emission. Various molecular interactions, namely, excited state reactions, molecular rearrangements, transfer of energy, and static and dynamic quenching, lead to fluorescence quenching. The binding mechanism of the ligand with the protein is usually delineated using the intrinsic fluorescence quenching of the protein.[28,29]

Table 1. MMGBSA Free Energy Estimate for HSA−GAL Binding

energy factors	average	standard deviation	std error of mean
VDWAALS	−35.6827	2.4231	0.0938
EEL	−95.7606	14.5083	0.5618
EGB	122.3907	14.0561	0.5443
ESURF	−4.1554	0.3504	0.0136
ΔG_{gas}	−131.4433	14.5967	0.5652
ΔG_{solv}	128.2353	14.1596	0.5483
ΔG (total)	−16.20	3.3340	0.1291

In the present work, the effect of GAL binding on the fluorescence spectroscopy of HSA was investigated (Figure 6). We observed a progressive decrease in the HSA fluorescence intensity with a corresponding increase in GAL concentration. HSA has a single Trp (Trp-214), and these observations suggested that after the binding of GAL, the microenvironment of Trp-214 becomes less hydrophobic than before. The obtained quenching data was used in the modified Stern−Volmer equation (MSV) to explore various binding parameters. Figure 6B shows the MSV plot of the HSA−GAL system; this plot's intercept gives the binding constant (K), and the slope gives the value of binding sites (n). The binding constant obtained for the HSA−GAL system was 4.39×10^4 M^{-1}, implying that this interaction was significant and revealing that significant interaction between HSA and GAL was responsible for the quenching mechanism. The binding site estimated from the slope of this plot was near unity. The magnitude of the binding constant was in line with the values that have been reported earlier for other ligand complexes of serum albumin,[28,30] highlighting the significance of this binding. Altogether, molecular docking, MD simulation studies, and fluorescence binding suggested that GAL−HSA forms a stable complex.

2.5. Isothermal Titration Calorimetry. After confirming the binding of GAL with HSA through computational approaches and fluorescence binding, isothermal titration calorimetry (ITC) was deployed to ascertain the binding energetics of the system and decipher the associated thermodynamic parameters with the binding. ITC reveals the molecular forces that are involved in the binding process. The heat released or absorbed in the sample cell due to the formation or dissociation of the protein−ligand complex is measured with respect to a reference cell filled with buffer. The obtained isotherm (Figure 7) advocates the spontaneous binding of GAL with HSA. The upper panel (each peak in the isotherm) corresponds to a single injection of GAL into the HSA solution. In contrast, the lower panel depicts the integrated plot of heat released per injection as a function of the molar ratio of ligand to protein. The number of binding sites (n), binding constant (K), enthalpy change (ΔH), and entropy change (ΔS) were determined directly by curve

https://doi.org/10.1021/acsomega.2c04004
ACS Omega 2022, 7, 34370−34377

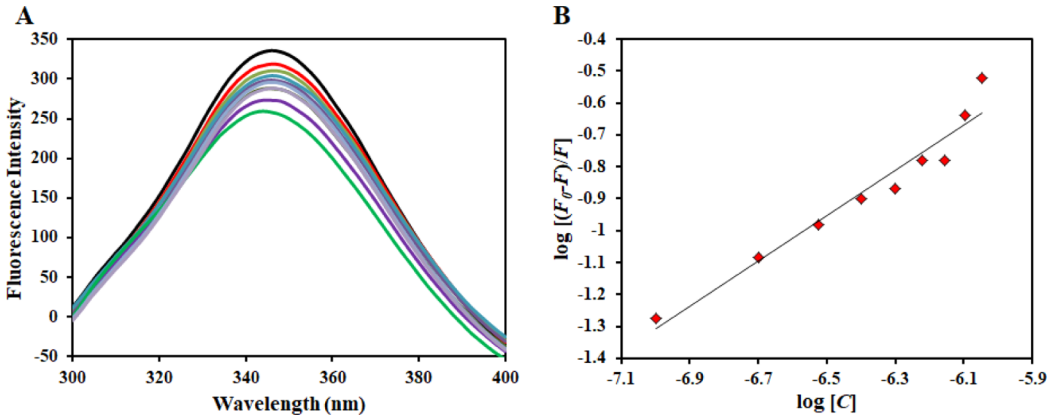

Figure 6. Fluorescence-based binding. (A) Intrinsic fluorescence quenching of HSA with increasing GAL concentration. (B) MSV plot of HSA–GAL system.

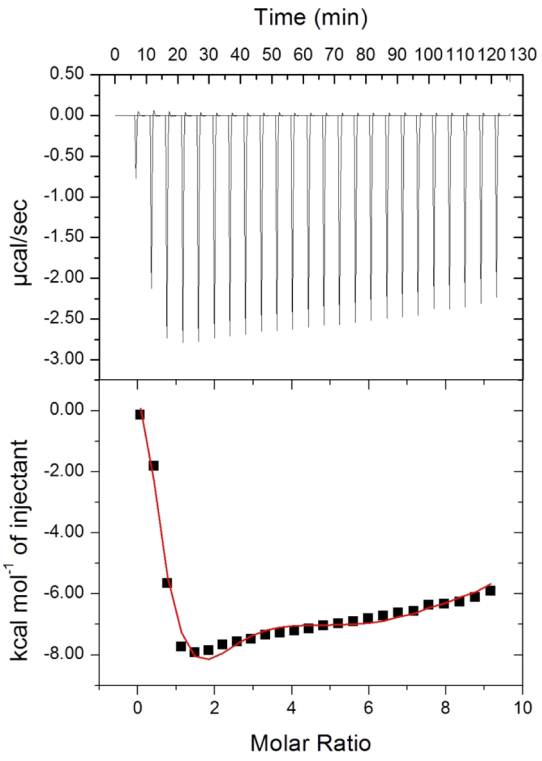

Figure 7. ITC profile of the HSA–GAL system. The sample cell was filled with 20 μM HSA, while the syringe contained 500 μM GAL.

fitting.[2] It is evident from the ITC isotherm that negative heat deflection is obtained, implying the binding to be exothermic. Table 2 gives the associated binding and thermodynamic parameters of the HSA–GAL system.

3. MATERIALS AND METHODS

3.1. Materials. HSA and GAL were procured from Sigma-Aldrich (St. Louis, USA). Sodium phosphate monobasic and dibasic were procured from Himedia. Prior to any experiment, HSA was dialyzed to remove excessive salts. Initially, we made a stock solution of HSA (75 μM) in 20 mM sodium phosphate buffer, pH 7.4. From this stock, a 4 μM working solution was made for the fluorescence experiment. For GAL, we prepared a 1 mM stock, and the dilution was done for the corresponding solutions. We used double distilled water for the preparation of all the buffers.

3.2. Molecular Descriptors. GAL was washed in a Molecular Operating Environment (MOE2020)[31] at pH = 7.3; few vital descriptors were calculated. GAL satisfies Lipinski drug-likeness test and is water soluble. Some critical molecular descriptors of GAL are mentioned in Table S1.

3.3. Molecular Docking. We retrieved the crystal structure for the HSA–Idarubicin complex from the Protein Data Bank (PDB ID: 6YG9). The X-ray crystal structure was stripped of all non-protein atoms and then prepped at a physiological pH of 7.2. Using the structure preparation tool in MOE2020, we fine-tuned the hydrogen bond networks and evaluated the protomeric states of histidine. Some residues were optimized for double protonated histidine protomer, one was protonated at delta nitrogen position (HID), and all Gln and Asn were optimized for proper hydrogen bonding.

The ligand GAL raw three-dimensional sdf file was downloaded from PubChem resource (https://pubchem.ncbi.nlm.nih.gov/compound/Galantamine). We followed the standard docking protocol, AutoDock Vina,[32] as the centroid for the ligand docking site. The grid dimensions were set to blind space in X, Y, and Z directions, with exhaustiveness parameters set to 50. We used the energy cut-off of 1 kcal/mol and the rmsd cutoff set to 2 Å. We kept the receptor rigid during the docking. For all other parameters, default settings were used. The top 2 poses of the docked complex were saved

Table 2. Thermodynamic and Binding Parameters Obtained from ITC

K_a (association constant), M^{-1}	ΔH (enthalpy change), cal/mol	ΔS (cal/mol/deg)
$K_{a1} = 1.14 \times 10^5 \pm 4.9 \times 10^3$	$\Delta H_1 = 729.6 \pm 311$	$\Delta S_1 = 25.6$
$K_{a2} = 2.38 \times 10^4 \pm 9.4 \times 10^2$	$\Delta H_2 = -6.15 \times 10^4 \pm 2.59 \times 10^3$	$\Delta S_2 = -186$
$K_{a3} = 1.08 \times 10^4 \pm 5.0 \times 10^2$	$\Delta H_3 = 9.817 \times 10^4 \pm 7.76 \times 10^3$	$\Delta S_3 = 348$
$K_{a4} = 1.41 \times 10^4 \pm 6.5 \times 10^2$	$\Delta H_4 = -1.820 \times 10^5 \pm 7.07 \times 10^3$	$\Delta S_4 = -591$

https://doi.org/10.1021/acsomega.2c04004
ACS Omega 2022, 7, 34370–34377

in the pdbqt format and then converted to the standard pdb format using AutoDock tools.[33] The top pose was chosen as the starting point for long-scale MD simulations.

3.4. System Preparation prior to MD Setup. We selected the top docked pose and subjected it to MD simulation for detailed analysis. Geometry optimization of the fragments using the B3LYP/6-31G(d) method[34] in the Gaussian 16 program[35] was done to find various ligand parameters. As reported in earlier studies, all other parameters were followed.[36] We followed a similar setup for both free HSA and HSA−GAL complex.

3.5. MD Simulation Details. We have employed GPU accelerated AMBER20 package for running the MDs simulation with HSA−GAL complex. Using the protocol as detailed in our previous publications,[37] we successfully probed the dynamics of both apo and GAL-bound HSA for 250 ns. Long-scale MD simulations are crucial to probe the protein motions atomistically, and we aimed for 250 ns as a traditional timescale to assess the complex. SHAKE was used, and a timestep of 2 fs was used in our simulation. Our previous publications inspired all the minimization, heating, equilibration stages, and final production.[36]

"We used the same protocol to simulate the free and complex forms of HSA for homogeneous results to accurately probe the intrinsic structural changes that occur upon GAL binding."

3.6. Fluorescence-Based Binding. We performed fluorescence-based binding on a Jasco FP-6200 spectrofluorometer (JAPAN). Fluorescence spectra were recorded in a quartz cuvette of path length 1 mm at 25 ± 0.1 °C, and the experiment was performed in triplicates. The protein was excited at 280 nm, and the emission was recorded in the 300−400 nm range with excitation and emission slit widths set at 10 nm. Titration was performed with increasing GAL concentration, and the attained data were interpreted with an MSV equation as per earlier published literature[38,39] to obtain different binding parameters. The protein concentration was fixed at 4 μM, while the ligand was titrated in the range of 0−0.9 μM.

3.7. Isothermal Titration Calorimetry. We performed an ITC experiment on MicroCal VP-ITC (Northampton, MA, USA) in accordance with earlier studies.[2,38] Initially, all the samples were degassed thoroughly to remove the bubbles, and post degassing, the sample cell was filled with the protein of interest, while the ligand was loaded into the rotator syringe. The sample cell contained 20 μM HSA, while the syringe was filled with 500 μM HSA. A programmed titration of 26 injections, in which the first injection of 2 μL is considered a false one, is followed by 10 μL injections, with stirring speed set at 307 rpm and spacing set at 280 s. Microcal Origin 8.0 plots the final figure and finds the associated binding and thermodynamic parameters: K_a, ΔG, ΔH, and ΔS.

4. DISCUSSION

Studies about drug plasma protein interactions are highly relevant in medicinal chemistry and emerging rapidly.[40] These decipher the mode of action of drugs unfolding their transport and distribution properties in the circulatory system.[41] Drugs' pharmacokinetics and pharmacodynamics are the two domains that need to be investigated to delineate the drug's mode of action. Thus, these play a crucial role in drug design and discovery. For pharmacological profiling, it is essential to understand the binding dynamics of the drugs with plasma proteins or target tissue proteins, thus highlighting the significance of studies involving the interaction of drugs with plasma proteins.[42,43]

HSA is arranged in three domains (i.e., I, II, and III), "encompassing amino acids 1−195, 196−383, and 384−585", respectively, with each domain made up of two separate helical subdomains (named A and B), which are linked by the random coil. There are two main binding sites for a multitude of diverse molecules, namely, "Sudlow's site I" (located in subdomain IIA) and site II (present in subdomain IIIA). Warfarin, an anticoagulant drug, is a stereotype ligand for Sudlow's site I, and ibuprofen, a non-steroidal anti-inflammatory agent, is regarded as a stereotypical ligand for Sudlow's site II.[44] Molecular docking is commonly deployed to understand the binding of the ligand with a protein, that is, to investigate various residues playing a crucial role in protein−ligand interaction.[45] The results suggested that GAL preferentially occupies the Sudlow site I, between domains IA and IIB of HSA, showing various essential residues involved in HSA−GAL binding.

Structural dynamics of the protein molecules are deciphered by examining the internal motions implicated in the protein's functionality.[46] MD simulation is a technique usually deployed to understand the internal motions and associated conformational changes observed upon binding of ligand to the protein under an obvious solvent environment.[47] In the present work, we carried out an all-atom extensive MD simulation (250 ns) to comprehend the conformational stability of the HSA−GAL complex. The analysis of rmsd, RMSF, R_g, and SASA trajectories discovered that GAL binding does not lead to significant conformational changes in HSA. The computational observations were warranted by a fluorescence binding experiment that provides the actual affinity of the ligand with a protein. Intrinsic fluorescence quenching of the proteins is generally deployed to understand the mechanism of its interaction with a ligand molecule.[28] The results showed a concomitant decrease in the fluorescence intensity with a corresponding increase in ligand concentration. Thus, fluorescence binding suggested that GAL binds to HSA with a significant affinity, forming a stable HSA−GAL complex. ITC is a sophisticated technique that deciphers the associated thermodynamic parameters of the protein−ligand system. ITC profile of the HSA−GAL system suggested the spontaneous binding of GAL with HSA, unveiling the associated thermodynamic parameters of the system. In conclusion, this study provided an insight into the binding mechanism of GAL with HSA.

5. CONCLUSIONS

The present study provides an atomistic insight into the binding of GAL with HSA, deciphering the detailed binding mechanism. Our results showed that GAL binds to HSA with a good affinity, forming a stable complex. It is well known that different ligands preferentially occupy Sudlow Site I (located in Subdomain IIA) or II (located in Subdomain IIIA). Molecular docking studies suggested that GAL binds in Sudlow's Site I located in Subdomain IIA. MD simulation studies further assessed the binding mechanism of GAL and also deciphered the dynamics of the HSA−GAL complex. GAL binds to HSA with a significant affinity, forming a stable complex. Thus, for the first time, this study demonstrates a detailed binding mechanism of GAL with HSA, establishing that GAL binds to HSA, forming a stable HSA−GAL complex.

https://doi.org/10.1021/acsomega.2c04004
ACS Omega 2022, 7, 34370−34377

■ ASSOCIATED CONTENT

Supporting Information

The Supporting Information is available free of charge at https://pubs.acs.org/doi/10.1021/acsomega.2c04004.

Molecular descriptors for ligands shown and alternative docked poses of Gal with HSA and selected interactions in a 2D plot (PDF)

■ AUTHOR INFORMATION

Corresponding Author

Ghulam Md Ashraf − *Pre-Clinical Research Unit, King Fahd Medical Research Center and Department of Medical Laboratory Sciences, Faculty of Applied Medical Sciences, King Abdulaziz University, Jeddah 21589, Saudi Arabia;* orcid.org/0000-0002-9820-2078; Email: anas.shamsi18@gmail.com

Authors

Debarati Das Gupta − *College of Pharmacy, University of Michigan, Ann Arbor, Michigan 48109, United States;* orcid.org/0000-0002-6289-5749

Mohammad Zubair Alam − *Pre-Clinical Research Unit, King Fahd Medical Research Center and Department of Medical Laboratory Sciences, Faculty of Applied Medical Sciences, King Abdulaziz University, Jeddah 21589, Saudi Arabia*

Saleh Salem Baeesa − *Division of Neurosurgery, College of Medicine, King Abdulaziz University, Jeddah 21589, Saudi Arabia;* orcid.org/0000-0002-3053-7912

Badrah S. Alghamdi − *Pre-Clinical Research Unit, King Fahd Medical Research Center, Department of Physiology, Faculty of Medicine, and The Neuroscience Research Unit, Faculty of Medicine, King Abdulaziz University, Jeddah 21589, Saudi Arabia*

Firoz Anwar − *Department of Biochemistry, Faculty of Science, King Abdulaziz University, Jeddah 21589, Saudi Arabia*

Thamer M. A. Alqurashi − *Department of Pharmacology, Faculty of Medicine, King Abdul-Aziz University, Rabigh 25724, Saudi Arabia*

Waleed Al Abdulmonem − *Department of Pathology, College of Medicine, Qassim University, Buraydah 52571, Saudi Arabia*

Mohammed A. Alyousef − *Division of Neurosurgery, King Abdulaziz University Hospital, Jeddah 21589, Saudi Arabia*

Fahad A. Alhumaydhi − *Department of Medical Laboratories, College of Applied Medical Sciences, Qassim University, Buraydah 52571, Saudi Arabia;* orcid.org/0000-0002-0151-8309

Anas Shamsi − *Centre for Interdisciplinary Research in Basic Sciences, Jamia Millia Islamia, New Delhi 110025, India; Centre of Medical and Bio-Allied Health Sciences Research, Ajman University, Ajman, United Arab Emirates;* orcid.org/0000-0001-7055-7056

Complete contact information is available at: https://pubs.acs.org/10.1021/acsomega.2c04004

Author Contributions

G.M.A.: Conceptualization, writing−review and editing, project administration, data analysis, investigation; D.D.G.: data curation, data validation, resources, visualization, software, writing−review and editing; M.Z.A.: Data validation, data analysis; writing−review and editing; S.S.B.: Methodology, investigation, writing−review and editing; B.S.A.: Editing, data curation; F.A.: Visualization, software, data validation, writing−review and editing; S.E.S.: Data curation, methodology; W.A.A.: Visualization, resources; T.M.A.A.: Data validation, software, writing−original draft, M.A.A.: Funding acquisition, data validation, methodology; A.S.: Visualization, software, writing−review and editing; A.I.: Data validation, software, resources, formal analysis.

Notes

The authors declare no competing financial interest.

■ ACKNOWLEDGMENTS

The authors extend their appreciation to the Deputyship for Research & Innovation, Ministry of Education in Saudi Arabia, for funding this research work through the project number "IFPRC-196-141-2020" and King Abdulaziz University, DSR, Jeddah, Saudi Arabia.

■ REFERENCES

(1) Singh, S. S. Preclinical pharmacokinetics: an approach towards safer and efficacious drugs. *Curr. Drug Metabol.* **2006**, *7*, 165−182.

(2) Alhumaydhi, F. A.; Aljasir, M. A.; Aljohani, A. S.; Alsagaby, S. A.; Alwashmi, A. S.; Shahwan, M.; Hassan, M. I.; Islam, A.; Shamsi, A. Probing the interaction of memantine, an important Alzheimer's drug, with human serum albumin: In silico and in vitro approach. *J. Mol. Liq.* **2021**, *340*, 116888.

(3) Bteich, M. An overview of albumin and alpha-1-acid glycoprotein main characteristics: highlighting the roles of amino acids in binding kinetics and molecular interactions. *Heliyon* **2019**, *5*, No. e02879.

(4) De Simone, G.; Pasquadibisceglie, A.; di Masi, A.; Buzzelli, V.; Trezza, V.; Macari, G.; Polticelli, F.; Ascenzi, P. Binding of direct oral anticoagulants to the FA1 site of human serum albumin. *J. Mol. Recognit.* **2021**, *34*, No. e2877.

(5) di Masi, A.; Leboffe, L.; Polticelli, F.; Tonon, F.; Zennaro, C.; Caterino, M.; Stano, P.; Fischer, S.; Hägele, M.; et al. Human serum albumin is an essential component of the host defense mechanism against Clostridium difficile intoxication. *J. Infect. Dis.* **2018**, *218*, 1424−1435.

(6) Alinovskaya, L. I.; Sedykh, S. E.; Ivanisenko, N. V.; Soboleva, S. E.; Nevinsky, G. A. How human serum albumin recognizes DNA and RNA. *Biol. Chem.* **2018**, *399*, 347−360.

(7) di Masi, A.; Trezza, V.; Leboffe, L.; Ascenzi, P. Human plasma lipocalins and serum albumin: Plasma alternative carriers? *J. Controlled Release* **2016**, *228*, 191−205.

(8) Pstras, L.; Waniewski, J.; Lindholm, B. Transcapillary transport of water, small solutes and proteins during hemodialysis. *Sci. Rep.* **2020**, *10*, 18736−12.

(9) Quinlan, G. J.; Martin, G. S.; Evans, T. W. Albumin: biochemical properties and therapeutic potential. *Hepatology* **2005**, *41*, 1211−1219.

(10) De Simone, G.; di Masi, A.; Ascenzi, P. Serum albumin: a multifaced enzyme. *Int. J. Mol. Sci.* **2021**, *22*, 10086.

(11) Gupta, D.; Lis, C. G. Pretreatment serum albumin as a predictor of cancer survival: a systematic review of the epidemiological literature. *Nutr. J.* **2010**, *9*, 1−16.

(12) Koga, M.; Kasayama, S. Clinical impact of glycated albumin as another glycemic control marker. *Endocr. J.* **2010**, *57* (9), 751−762.

(13) Sbarouni, E.; Georgiadou, P.; Voudris, V. Ischemia modified albumin changes−review and clinical implications. *Clin. Chem. Lab. Med.* **2011**, *49*, 177−84.

(14) Belinskaia, D. A.; Voronina, P. A.; Shmurak, V. I.; Vovk, M. A.; Batalova, A. A.; Jenkins, R. O.; Goncharov, N. V. The universal soldier: Enzymatic and non-enzymatic antioxidant functions of serum albumin. *Antioxidants* **2020**, *9*, 966.

(15) Liberati, A.; Moja, L.; Moschetti, I.; Gensini, G. F.; Gusinu, R. Human albumin solution for resuscitation and volume expansion in critically ill patients. *Intern. Emerg. Med.* **2006**, *1*, 243−245.

(16) Spinella, R.; Sawhney, R.; Jalan, R. Albumin in chronic liver disease: structure, functions and therapeutic implications. *Hepatol. Int.* **2016**, *10*, 124−132.
(17) Khan, A.; Khan, F.; Shahwan, M.; Khan, M. S.; Husain, F. M.; Rehman, M. T.; Hassan, M. I.; Islam, A.; Shamsi, A. Mechanistic insight into the binding of graphene oxide with human serum albumin: Multispectroscopic and molecular docking approach. *Spectrochim. Acta, Part A* **2021**, *256*, 119750.
(18) Bhattacharya, A. A.; Curry, S.; Franks, N. P. Binding of the general anesthetics propofol and halothane to human serum albumin: high resolution crystal structures. *J. Biol. Chem.* **2000**, *275*, 38731−38738.
(19) Sudlow, G.; Birkett, D.; Wade, D. The characterization of two specific drug binding sites on human serum albumin. *Mol. Pharmacol.* **1975**, *11*, 824−32.
(20) Walczak-Nowicka, J.; Herbet, M. Acetylcholinesterase Inhibitors in the Treatment of Neurodegenerative Diseases and the Role of Acetylcholinesterase in their Pathogenesis. *Int. J. Mol. Sci.* **2021**, *22*, 9290.
(21) Liu, P.-P.; Xie, Y.; Meng, X.-Y.; Kang, J.-S. History and progress of hypotheses and clinical trials for Alzheimer's disease. *Signal Transduct. Targeted Ther.* **2019**, *4*, 1−22.
(22) Mufson, E. J.; Counts, S. E.; Perez, S. E.; Ginsberg, S. D. Cholinergic system during the progression of Alzheimer's disease: therapeutic implications. *Expert Rev. Neurother.* **2008**, *8*, 1703−1718.
(23) Kowal, N. M.; Ahring, P. K.; Liao, V. W.; Indurti, D. C.; Harvey, B. S.; O'Connor, S. M.; Chebib, M.; Olafsdottir, E. S.; Balle, T. Galantamine is not a positive allosteric modulator of human $\alpha4\beta2$ or $\alpha7$ nicotinic acetylcholine receptors. *Br. J. Pharmacol.* **2018**, *175*, 2911−2925.
(24) Burns, A.; Bernabei, R.; Bullock, R.; Jentoft, A. J. C.; Frölich, L.; Hock, C.; Raivio, M.; Triau, E.; Vandewoude, M.; et al. Safety and efficacy of galantamine (Reminyl) in severe Alzheimer's disease (the SERAD study): a randomised, placebo-controlled, double-blind trial. *Lancet Neurol.* **2009**, *8*, 39−47.
(25) Hager, K.; Baseman, A. S.; Nye, J. S.; Brashear, H. R.; Han, J.; Sano, M.; Davis, B.; Richards, H. M. Effects of galantamine in a 2-year, randomized, placebo-controlled study in Alzheimer's disease. *Neuropsychiatric Dis. Treat.* **2014**, *10*, 391.
(26) Anwar, S.; Shamsi, A.; Kar, R. K.; Queen, A.; Islam, A.; Ahmad, F.; Hassan, M. I. Structural and biochemical investigation of MARK4 inhibitory potential of cholic acid: Towards therapeutic implications in neurodegenerative diseases. *Int. J. Biol. Macromol.* **2020**, *161*, 596−604.
(27) Anwar, S.; Shamsi, A.; Shahbaaz, M.; Queen, A.; Khan, P.; Hasan, G. M.; Islam, A.; Alajmi, M. F.; Hussain, A.; et al. Rosmarinic acid exhibits anticancer effects via MARK4 inhibition. *Sci. Rep.* **2020**, *10*, 10300.
(28) Rehman, M. T.; Shamsi, H.; Khan, A. U. Insight into the binding mechanism of imipenem to human serum albumin by spectroscopic and computational approaches. *Mol. Pharm.* **2014**, *11*, 1785−1797.
(29) Eftink, M. R.; Ghiron, C. A. Fluorescence quenching studies with proteins. *Anal. Biochem.* **1981**, *114*, 199−227.
(30) Shamsi, A.; Mohammad, T.; Anwar, S.; Alajmi, M. F.; Hussain, A.; Hassan, M. I.; Ahmad, F.; Islam, A. Probing the interaction of Rivastigmine Tartrate, an important Alzheimer's drug, with serum albumin: Attempting treatment of Alzheimer's disease. *Int. J. Biol. Macromol.* **2020**, *148*, 533−542.
(31) Nazouri, A.-S.; asadpour, O.; Dabiri, S.; Pourseyedi, B.; Lashkarizadeh, M. R.; Zeinalyneghad, H. High expression of sphingosine kinase 1 in estrogen and progesterone receptors-negative breast cancer. *Iran. J. Pathol.* **2017**, *12*, 218.
(32) Trott, O.; Olson, A. J. AutoDock Vina: improving the speed and accuracy of docking with a new scoring function, efficient optimization, and multithreading. *J. Comput. Chem.* **2010**, *31*, 455.
(33) Forli, S.; Huey, R.; Pique, M. E.; Sanner, M. F.; Goodsell, D. S.; Olson, A. J. Computational protein-ligand docking and virtual drug screening with the AutoDock suite. *Nat. Protoc.* **2016**, *11*, 905−919.
(34) Bayly, C. I.; Cieplak, P.; Cornell, W.; Kollman, P. A. A well-behaved electrostatic potential based method using charge restraints for deriving atomic charges: the RESP model. *J. Phys. Chem.* **1993**, *97*, 10269−10280.
(35) Frisch, M. J.; Trucks, G. W.; Schlegel, H. B.; Scuseria, G. E.; Robb, M. A.; Cheeseman, J. R.; Scalmani, G.; Barone, V.; Petersson, G. A.; et al. *Gaussian*, Revision C.01; Gaussian, Inc.: Wallingford, CT, 2016.
(36) Anwar, S.; DasGupta, D.; Azum, N.; Alfaifi, S. Y.; Asiri, A. M.; Alhumaydhi, F. A.; Alsagaby, S. A.; Sharaf, S. E.; Shahwan, M.; et al. Inhibition of PDK3 by artemisinin, a repurposed antimalarial drug in cancer therapy. *J. Mol. Liq.* **2022**, *355*, 118928.
(37) Anwar, S.; DasGupta, D.; Shafie, A.; Alhumaydhi, F. A.; Alsagaby, S. A.; Shahwan, M.; Anjum, F.; Al Abdulmonem, W.; Sharaf, S. E.; et al. Implications of Tempol in Pyruvate Dehydrogenase Kinase 3 Targeted Anticancer therapeutics: Computational, Spectroscopic and Calorimetric Studies. *J. Mol. Liq.* **2022**, *350*, 118581.
(38) Shamsi, A.; Anwar, S.; Mohammad, T.; Alajmi, M. F.; Hussain, A.; Rehman, M.; Hasan, G. M.; Islam, A.; Hassan, M. MARK4 inhibited by AChE inhibitors, donepezil and Rivastigmine tartrate: insights into Alzheimer's disease therapy. *Biomolecules* **2020**, *10*, 789.
(39) Khan, M. S.; Shahwan, M.; Shamsi, A.; Alhumaydhi, F. A.; Alsagaby, S. A.; Al Abdulmonem, W.; Abdullaev, B.; Yadav, D. K. Elucidating the Interactions of Fluoxetine with Human Transferrin Employing Spectroscopic, Calorimetric, and In Silico Approaches: Implications of a Potent Alzheimer's Drug. *ACS Omega* **2022**, *7*, 9015.
(40) Nusrat, S.; Siddiqi, M. K.; Zaman, M.; Zaidi, N.; Ajmal, M. R.; Alam, P.; Qadeer, A.; Abdelhameed, A. S.; Khan, R. H. A comprehensive spectroscopic and computational investigation to probe the interaction of antineoplastic drug nordihydroguaiaretic acid with serum albumins. *PLoS One* **2016**, *11*, No. e0158833.
(41) Yang, F.; Yue, J.; Ma, L.; Ma, Z.; Li, M.; Wu, X.; Liang, H. Interactive associations of drug−drug and drug−drug−drug with IIA subdomain of human serum albumin. *Mol. Pharm.* **2012**, *9*, 3259−3265.
(42) Abdelhameed, A. S.; Nusrat, S.; Ajmal, M. R.; Zakariya, S. M.; Zaman, M.; Khan, R. H. A biophysical and computational study unraveling the molecular interaction mechanism of a new Janus kinase inhibitor Tofacitinib with bovine serum albumin. *J. Mol. Recognit.* **2017**, *30*, No. e2601.
(43) Shamsi, A.; Ahmed, A.; Bano, B. Probing the interaction of anticancer drug temsirolimus with human serum albumin: Molecular docking and spectroscopic insight. *J. Biomol. Struct. Dyn.* **2018**, *36*, 1479−1489.
(44) Fasano, M.; Curry, S.; Terreno, E.; Galliano, M.; Fanali, G.; Narciso, P.; Notari, S.; Ascenzi, P. The extraordinary ligand binding properties of human serum albumin. *IUBMB Life* **2005**, *57*, 787−796.
(45) Shamsi, A.; Shahwan, M.; Alhumaydhi, F. A.; Alwashmi, A. S.; Aljasir, M. A.; Alsagaby, S. A.; Al Abdulmonem, W.; Hassan, M. I.; Islam, A. Spectroscopic, calorimetric and in silico insight into the molecular interactions of Memantine with human transferrin: Implications of Alzheimer's drugs. *Int. J. Biol. Macromol.* **2021**, *190*, 660−666.
(46) Wang, J.-F.; Chou, K.-C. Insight into the molecular switch mechanism of human Rab5a from molecular dynamics simulations. *Biochem. Biophys. Res. Commun.* **2009**, *390*, 608−612.
(47) Mohammad, T.; Khan, F. I.; Lobb, K. A.; Islam, A.; Ahmad, F.; Hassan, M. I. Identification and evaluation of bioactive natural products as potential inhibitors of human microtubule affinity-regulating kinase 4 (MARK4). *J. Biomol. Struct. Dyn.* **2019**, *37*, 1813−1829.

https://doi.org/10.1021/acsomega.2c04004
ACS Omega 2022, 7, 34370−34377